Interaction between physical heterogeneity and microbial processes in subsurface sediments: a laboratory-scale column experiment

Journal:	*Environmental Science & Technology*
Manuscript ID	es-2016-06506h.R2
Manuscript Type:	Article
Date Submitted by the Author:	03-May-2017
Complete List of Authors:	Perujo, N.; Universitat Politècnica de Catalunya (UPC), Department of Civil and Environmental Engineering. Associated Unit: Hydrogeology Group (UPC-CSIC); Universitat de Girona, GRECO-Institut d'Ecologia Aquàtica Sanchez-Vila, X.; Universitat Politècnica de Catalunya (UPC), Department of Civil and Environmental Engineering. Associated Unit: Hydrogeology Group (UPC-CSIC) Proia, L.; Universitat de Girona, GRECO-Institut d'Ecologia Aquàtica Romaní, A.; Universitat de Girona, GRECO-Institut d'Ecologia Aquàtica

Interaction between physical heterogeneity and microbial processes in subsurface sediments: a laboratory-scale column experiment

N. Perujo[a,b,c,*], X. Sanchez-Vila[a,b], L. Proia[c] A.M. Romaní[c]

[a] Department of Civil and Environmental Engineering, Universitat Politècnica de Catalunya (UPC), Jordi Girona 1-3, 08034 Barcelona, Spain

[b] Associated Unit: Hydrogeology Group (UPC-CSIC)

[c] GRECO - Institute of Aquatic Ecology, Universitat de Girona, Girona, Spain

*Corresponding author, e-mail address: nuria.perujo@upc.edu

Abstract

Physical heterogeneity determines interstitial fluxes in porous media. Nutrients and organic matter distribution in depth influence physicochemical and microbial processes occurring in subsurface. Columns 50 cm long were filled with sterile silica sand following 5 different setups combining fine and coarse sands or a mixture of both mimicking potential water treatment barriers. Water was supplied continuously to all columns during 33 days. Hydraulic conductivity, nutrients and organic matter, biofilm biomass and activity were analysed in order to study the effect of spatial grain size heterogeneity on physicochemical and microbial processes and their mutual interaction. Coarse sediments showed higher biomass and activity in deeper areas compared to the others; however, they resulted in incomplete denitrification, large proportion of dead bacteria in depth, and low functional diversity. Treatments with fine sediment in the upper 20 cm of the columns showed high phosphorous retention. However, low hydraulic conductivity values reported in these sediments seemed to constraint biofilm activity and biomass. On the other hand, sudden transition from coarse-to-fine grain sizes promoted a hot-spot of organic matter degradation and biomass growth at the

interface. Our results reinforce the idea that grain-size disposition in subsurface sandy sediments drives the interstitial fluxes, influencing microbial processes.

TOC Art

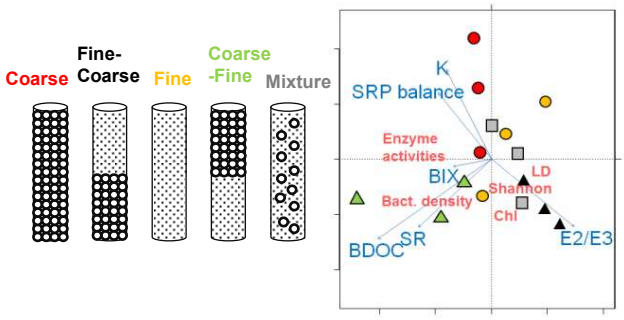

Keywords: sediment heterogeneity, infiltration columns, hydraulic conductivity, biofilm biomass, hot-spots, microbial processes

1. Introduction

Bacterial communities inhabiting surface and subsurface sediments catalyse a number of ecosystem processes, including uptake, storage and mineralization of dissolved organic matter, as well as assimilation of inorganic nutrients.[1,2] Processes occurring in subsurface sediments are not only relevant in natural environments (such as in river hyporheic zones), but also in man-made applications for water quality improvement (such as land based wastewater disposal or managed aquifer recharge facilities). Infiltration systems are water treatment systems that rely on water percolation[3] through a porous medium whereby the quality of the effluent improves progressively during the infiltration path as a consequence of the combination of biological, chemical and physical processes[4,5] driven by microbial activity[6] at the cost of progressively reducing infiltration rates.[7] In this sense, infiltration systems may be advantageous in many aspects; they may increase (by recharge) groundwater supplies, provide further treatment to infiltrating water, and reduce degradation of stream-water quality.[8] Infiltration systems may also enable water reuse thereby

preserving valuable freshwater resources.[9] Some examples of infiltration systems are Rapid Infiltration Basin Systems (RIBS), Slow Sand Filtration Systems (SSFS), Soil-Aquifer treatment (SAT) among others.

Biofilms colonizing subsurface sediments offer the potential for biotransformation of organic compounds, thereby providing an in situ method for treating contaminated groundwater supplies,[10] also relevant for emerging compounds degradation.[11] Processing by extracellular enzymes is the primary mechanism for the microbial degradation of polymeric and macromolecular organic matter into low-molecular-weight molecules which can then cross bacterial cell membranes, becoming available for bacterial growth and nutrient cycles.[12] Extracellular enzyme activities are good proxies to determine nutrient demands and decomposition capabilities of microorganisms, as well as to characterize the quantity and quality of available dissolved organic carbon and nutrients in the environment.[12]

Heterotrophic bacteria assimilate dissolved organic carbon (DOC) and concomitantly release substantial amounts of carbon in the form of extracellular polymeric substances (EPS).[13] The EPS layer traps and stores particulates and nutrients for cell metabolism and is generally thought to comprise the major component of bacterial biofilm.[14] It can also affect the physical characteristics of porous medium through the reduction of available pore spaces for flow and alteration of water retention,[15-16] significantly reducing hydraulic conductivity and enhancing dispersion of solutes.[17] Microbial processes and biomass accrual in subsurface sediments are determined by the surrounding physical and chemical conditions. The link between physicochemical and biological parameters is complex[18,19] but the consideration of the interactions of soil microorganisms with their physical and chemical environments is crucial for substantially advance in our understanding of microbial ecology.[19-21] Recently, some studies addressed water quality changes resulting from infiltration in porous media[3,5] and biofilm accumulation in infiltration systems (a term called bioclogging).[22] Link

between physicochemical and biological processes in porous media has also been studied by other authors.[14,19,20,23,24,25]

Spatial heterogeneity of particle grain sizes distribution determines the specific physical and chemical conditions in subsurface sediments. Sediment grain size and distribution are key parameters determining interstitial fluxes, which also modulate the distribution of electron donors and acceptors and, consequently, the distribution of microbial processes in subsurface sediments.[26,] Related to this, Higashino[27] proposed a model where grain diameter plays an important role in determining both hydraulic conductivity and microbial oxygen uptake rate. Small hydraulic conductivity resulted in small dissolved oxygen transfer but large microbial oxygen uptake rate. In coarse sand they stated that even dissolved oxygen transfer rate can be large owing to a large hydraulic conductivity, microbial oxygen uptake rate is small since available surface area for colonization by biofilms is reduced. On the other hand, Essandoh, Tizaoui and Mohamed[28] concluded that the type of soil affects the performance of soil columns; specifically they stated that low hydraulic conductivity results in low microbial growth and low DOC removal. Similarly, Dodds, Randel and Edler[29] stated that microbial activity may be greatest with the largest particle size because of increased water exchange through pores, and smallest particle size would promote denitrification.

As the influence of substratum type or grain size on biogeochemical processes and biofilm accumulation is not clear and it remains poorly understood, further investigation is needed to focus on the interaction between physicochemical and biological parameters in different spatial grain size distributions. The present work addresses the link between physicochemical and microbial processes in subsurface sediments using laboratory-scale infiltration columns of different sediment grain sizes and distribution. The objectives are to understand the influence of subsurface sediment heterogeneity on (1) physicochemical water parameters; (2) biofilm biomass and activity and (3) the relationship between these parameters and how they influence biogeochemical processes occurring in sediment infiltration systems. For this purpose, we designed a number of column setups (mimicking potential

sand filter treatments) with different combinations of fine and coarse sands placed in different columns.

We expected that coarse sediment would display higher infiltration rates, which would transfer higher quantity of dissolved oxygen (DO), nutrients and organic matter during the infiltration process. This will promote biofilm activity and biomass in deeper areas in columns having coarse sediment. On the other hand, low hydraulic conductivity in fine sediments would promote anaerobic zones potential to denitrification processes, but biofilm activity and biomass in depth will be limited due to reduced transport of nutrients and organic matter in depth. Also we expect high phosphorous retention in fine sediments compared to coarse ones. Mixture of coarse and fine sand would enable the coexistence of slow and rapid zones which would promote aerobic and anaerobic processes at the same layers, as well as enhancing biogeochemical processes and biomass development which could be responsible of stronger bioclogging. Bilayer columns of coarse sediment in the upper part and fine sediment in the bottom part would take advantage of high transfer of DO, nutrients and organic matter in the coarse layer, and anaerobic conditions and phosphorous retention in the fine layer.

2. Experimental

2.1 Experimental design and sampling

The laboratory experiment consisted in flow-through columns filled with sediments of different grain sizes. We used two different grain sizes: coarse sand (0.9 – 1.2 mm) and fine sand (0.075 – 0.250 mm), placed in columns 50 cm long and 4.6 cm diameter to create 5 treatments (3 replicate per treatment for a total of 15 columns) with different spatial distribution of fine and coarse sand. All the sand had been previously burned (450 ºC for 4 hours) and cleaned with distilled water to ensure it was free from organic matter.

We designed a column setup (mimicking potential sand filter treatments) with five combinations of fine and coarse sands (see Fig. 1). Each column was filled to a height of 40 cm. A layer of 10 cm of

115 water was left above the sediment surface. Infiltration was performed with synthetic water (13 mg·L^{-1}
116 Na_2SO_4, 16.1 mg·L^{-1} Na_2SiO_3, 29.4 mg·L^{-1} $CaCl_2$*$2H_2O$, 0.6 mg·L^{-1} KCl, 3 mg·L^{-1} $MgSO_4$*$7H_2O$,
117 26.5 mg·L^{-1} Na_2CO_3, 0.6 mg·$L^{-1}$$NH_4H_2PO_4$, 7.3 mg·$L^{-1}$ $(NH_4)(NO_3)$, and 4.27 mg·L^{-1} humic acids in
118 MQ water) reproducing the chemical signature of a well characterized pristine river (Fuirosos stream,
119 Spain).[30] Nutrient and organic matter concentrations where slightly enhanced to facilitate biofilm
120 colonization of the sediment. An inlet water tank (50 L) was placed on top of each group of 5
121 columns to produce a flow-through system. Water tanks were refilled when necessary to ensure
122 continuous infiltration. The experiment was performed at a constant temperature (20 ºC) with a 12:12
123 light:dark cycle (incident light was 130-150 μmol photons·m^{-2}·s^{-1}). The portion of the columns filled
124 with sand was kept in the dark to mimic subsurface conditions by wrapping them with opaque
125 material. Light conditions were allowed in the surface sediment as in real infiltration sand basins. At
126 the start of the experiment, a bacterial inoculum extracted from natural sediment (from Fuirosos
127 stream) was added to all the columns (700 ml, $1.27 \cdot 10^7$ cel·ml^{-1}).

128 During the 33 days of experiment, physical and chemical water characteristics (pH, DO, conductivity
129 and temperature) were measured twice per week in the inlet tanks to ensure homogeneous conditions
130 during all the experiment. Water samples from the inlet tanks and the outlet of each of the columns
131 were taken on days 15, 20, 30 and 33 to measure dissolved nutrients and organic matter content
132 (nitrates/nitrites, ammonium, phosphates, dissolved organic carbon –DOC-, and several dissolved
133 organic matter –DOM- quality properties). DO in sediment at three different depths and flow at the
134 outlet of the columns, were measured weekly. All measurements were performed during the light
135 cycle and at the same time (after 6 hours of the start of the light conditions) to reduce variability
136 between measurements due to day/night cycles.

137 At the end of the experiment, columns were dismantled for sediment biofilm biomass and activity
138 measurements at three different depths (0-2 cm, 18-22 cm, 36-38 cm). These depths corresponded to
139 the top (inlet) and the bottom (outlet) of the column, and an intermediate point which in two of the

configurations correspond to the interface between coarse and fine grain sizes. Sediment samples were analysed for bacterial density, bacterial viability, chlorophyll-a content –chl-a- , extracellular polymeric substances –EPS- content, extracellular enzyme activity and functional diversity. Each layer of sediment was sampled totally and homogenized. Sub-samples of 1ml of sediment were then collected using an uncapped syringe.

2.2 Physical and chemical water analyses

2.2.1 Flow and hydraulic conductivity

Flow rate (Q) was measured manually at the outlet of each individual column. Hydraulic conductivity K (in cm/s) was calculated using Darcy's law:

$$K = \frac{Q\,L}{\Delta h\,A} \quad (1)$$

where Δh is the piezometric head difference (set at a constant value of 1108 ± 9 cm), L is total length of the sediment (= 40 cm), A is the cross-section area (= 16.619 cm^2), and Q is measured in cm^3/s.

Advection time is a measure of the time that takes water to go through the sediment. Advection time (t) was calculated using the formula:

$$t = (Ø \cdot L \cdot A) / Q \quad (2)$$

where Ø is the porosity of the sediment (0.4 for the coarse sediment and 0.32 for the fine sediment).

158 *2.2.2 Chemical water analyses*

159 Physicochemical water parameters (pH, DO, conductivity and temperature) were measured with
160 specific probes (HQd Field Case, HACH) in the supply tanks. To measure DO at different depths
161 (surface, 20 cm and 40 cm) without perturbing the sediment biofilm, a non-invasive method was used
162 by fixing oxygen sensor spots inside the wall of the columns and measuring dissolved oxygen
163 concentration using an optical fiber (PreSens).

164 Samples for dissolved nutrients and organic matter determination were filtered in pre-burned (4
165 hours, 450ºC) filters (GF/F, 0.7 µm, Whatmann). After filtering, samples for dissolved inorganic
166 nutrients were frozen until analysis. DOM spectroscopic properties were analysed in fresh. Samples
167 for DOC analysis were acidified and kept at 4ºC until analysis. Inorganic nutrients were analysed as
168 following: nitrate by ionic chromatography (761 Compact IC 1.1 Metrohm), phosphate by the
169 Murphy-Riley[31] spectrophotometric method, and ammonium by the spectrophotometric sodium
170 salicylate protocol.[32] DOC was analysed with TOC-V CHS/TNM-1 SHIMADZU. Spectroscopic
171 properties were analysed in order to characterize potential changes in DOM quality and included the
172 following parameters: the Slope ratio (SR) described in Helms et al.[33] which is inversely correlated to
173 organic matter molecular weight; the Fluorescence Index (FI) described in Cory and Mcknight[34]
174 indicative of the origin of the organic matter; the Biological Index (BIX, Huguet et al.)[35] as indicator
175 of recent biological activity and the E2/E3 index which is related to photo reactivity (Minero et al.).[36]
176 Biodegradable dissolved organic carbon (BDOC) was analysed once, following the protocol
177 described by Servais et al.[37]

178 **2.3 Sediment biofilm biomass and activity**

179 ***2.3.1 Bacterial density***

180 Bacterial density was determined by flow cytometry (FACSCalibur, Becton Dickinson) following a
181 protocol adapted from Amalfitano et al.[38] Filter-sterilized (filtered by 0.2 µm) simplified synthetic
182 water (without nutrients and organic carbon, 10 ml) and formaldehyde (100 µl, 37%) were added to

each sediment sample. Samples were kept in the dark at room temperature until analysis. Sediment samples were sonicated for 1 minute, shook for 30 seconds, and sonicated again for 1 minute to extract the biofilm from sediment grains (Ultrasons, Selecta). A sub-sample of the obtained extract (1 ml) was pipetted into a glass vial and 9 ml of detaching solution was added. Detaching solution consists of NaCl (130mM), Na_2HPO_4 (7 mM), NaH_2PO_4 (3 mM), formaldehyde (37%), sodium pyrophosphate decahydrate 99% (0.1% final concentration), and tween 20 (0.5% final concentration), and it helps to separate cells avoiding aggregation. Samples were then shaken for 30 minutes (150 rpm) at dark and room temperature conditions. Samples were left 10 minutes at 4 ºC, and sonicated with ice during two cycles of 1 minute. After shaking for 1 minute, samples were left for 5 minutes for sedimentation of larger particles and 1 ml of supernatant was transferred in an Eppendorf. Nycodenz (1 ml) was added to the bottom of the Eppendorf and samples were centrifuged (14000 rpm) for 90 minutes at 4 ºC. Purified extract (400 µl) was stained with Syto13 (4µl Fisher, 5µM solution) and incubated in the dark for 30 minutes. Stained samples were counted using flow cytometry (FACSCalibur, Becton Dickinson). To normalize fluorescence data, a bead solution (10µl of 10^6 beads·ml^{-1}, Fisher 1.0 µm) was added to the samples in a known concentration. Results are reported as bacterial cells·10^6/g sediment dry weight.

2.3.2 Bacterial viability

A bacterial extract from fresh sediment samples was first prepared to obtain a homogeneous and dispersed cell suspension. Pyrophosphate (5ml, 50mM) was added to fresh sediment samples[39] and they were incubated for 15 minutes at room temperature and soft shaking. Samples were then sonicated for one minute with ice to avoid cell disruption.[40] A sub-sample of the obtained extract (1 ml) was diluted with filter-sterilized simplified synthetic water (1:50). A sub-sample of the diluted extract (400 µl) was stained with propidium iodide and Syto 9 (8 µl, BacLight Bacterial Viability Kit).[41] Syto 9 penetrates all bacterial membranes and stains the cells fluorescent green, while propidium iodide only penetrates cells with damaged membranes, and the combination of the two

208 stains produced red fluorescing cells.[42] Samples were incubated in the dark for 15 minutes. According
209 to Falcioni et al.[41] to normalize fluorescence data, a bead solution (40µl of 10^6 beads·ml^{-1}, Fisher 1.0
210 µm) was added to the samples in a known concentration. Bacterial viability was measured by flow
211 cytometry (FACSCalibur, Becton Dickinson). Results are reported as the ratio between live cells (L)
212 and dead cells (D) -LD ratio-.

213 ***2.3.3 Chlorophyll-a***

214 Samples for chl-a analysis were placed in glass vials and kept in dark at (-20ºC) until analysis. Chl-a
215 concentration was determined as described by Jeffrey and Humphrey[43]. Acetone 90% (10 ml) was
216 added to each sediment sample in order to extract the chl-a and kept in dark for 8-12 hours at 4ºC.
217 Sediment samples were sonicated and filtered (GF/C, 1.4 µm, 47 mm). Absorbance was measured at
218 430, 665, and 750 nm. Results are given as µg of chlorophyll-a/g sediment dry weight.

219 ***2.3.4 Content of polysaccharides in extracellular polymeric substances***

220 EPS were extracted by a cation exchange resin (CER) and the content of polysaccharides measured
221 spectrophotometrically following the protocol described by Dubois et al.[44] Sediment samples for EPS
222 analysis were placed in plastic flasks and frozen until analysis. Previous to analyses, CER (Dowex
223 Marathon C sodium form, Sigma-Aldrich) was conditioned with HCl (4M) and NaOH (1M)
224 following manufacturer instructions, and the samples were left to reach room temperature. Then,
225 samples were placed in an Eppendorf with 1ml of simplified synthetic water plus 0.3 g of CER. After
226 shaking them carefully, samples were incubated with ice for one hour in a shaker (250 rpm). Samples
227 were then centrifuged (11000 rpm) for 15 minutes at 4 ºC. The supernatant (500 µl) from each sample
228 was pipetted into glass tubes. A phenol solution (12.5 µl, 80% w/w) was added to the glass tubes.
229 After carefully shaken, 1.25 ml of H_2SO_4 (95.5%) was added to the samples. Glass tubes were
230 capped. After 10 minutes, samples were carefully shaken and incubated for 20 minutes in a water
231 bath (30 ºC). Absorbance (485 nm) was measured in a spectrophotometer. To determine EPS

concentration, a glucose standard was prepared. Further transformation of results to sediment dry weight was performed. Results are given in µg glucose-equivalents/g dry weight.

2.3.5 Extracellular enzyme activities

Extracellular enzyme activities β-glucosidase (EC 3.2.1.21), β-xylosidase (EC 3.2.1.37), phosphatase (EC 3.1.3.1 -2) and leucine-aminopeptidase (EC 3.4.11.1) were measured with spectrofluorometry using fluorescent-linked artificial substrates (Methylumbelliferyl (MUF)-β-D-glucopyranoside, MUF-β-D-xyloside, MUF-phosphate and L-leucine-7-amido-4-methylcoumarin hydrochloride (Leu-AMC), Sigma-Aldrich). All enzyme activities were measured under saturating conditions (0.3 mM).[45] Fresh sediment samples were placed in a 15 ml tube with synthetic water (4 ml) and 120µl of artificial substrate. A blank for each artificial substrate was prepared with synthetic water in order to determine the abiotic hydrolysis of the substrate itself. Samples and blanks were incubated for 1 hour in the dark with agitation. After 1-hour incubation, glycine buffer (4 ml, pH 10.4) was added in order to stop the reaction and maximize MUF and AMC fluorescence. Samples were centrifuged (2000 g) for 2 minutes, and the supernatant (350 µl) of each sample was placed into a 96 wells black plate (Greiner bio-one). Fluorescence was measured at excitation/emission wavelengths of 365/455 (MUF fluorescence) and 364/445 (AMC fluorescence) in a fluorimeter plate reader (Tecan, infinite M200 Pro). To determine extracellular enzyme activities, MUF and AMC standards were prepared and measured for their fluorescence. Results are given in nmol MUF/g dry weight·h or nmol AMC/g dry weight·h.

2.3.6 Functional diversity

Biolog Ecoplates microplates (AEX Chemunex) were used to determine functional diversity of sediment communities. Each microplate contains three replicate wells of 31 carbon sources and a blank (no substrate). To obtain an extract of the microbial community from the sediment samples a similar procedure to that used for bacteria viability was used. Pyrophosphate (5 ml, 50 mM) was added to the sediment samples which were then incubated for 15 minutes at room temperature and

soft shaking. Samples were sonicated for one minute with ice. A sub-sample of the obtained extract (1 ml) was diluted with filter-sterilized simplified synthetic water (1:50). Microplates were inoculated under sterile conditions with 130 µl of the diluted extract to each well and incubated in dark conditions at 20 ºC for 14 days. Absorbance was measured every 24 hours at 590 nm (Tecan, infinite M200 Pro). The color measured in each well, a measure of the capability of the inoculated community to metabolize the specific substrate, was corrected by the color measured in the blank well from each microplate. During the incubation, absorbance measurements increased following a sigmoidal pattern, and after 14 days of incubation the absorbance was saturated. Absorbance data of each substrate, when the average well color (AWCD) was 0.5, was used to calculate functional diversity by means of the Shannon diversity index.[46]

2.4 Data treatment

Normalized hydraulic conductivity with respect to the original value (K/K_0, K being actual hydraulic conductivity and K_0 the initial one at each column) was calculated as a function of time and analyzed with ANCOVA analysis. Oxygen balance was calculated from the differences between column outlets and inlets. To study the relationship between oxygen balance and normalized hydraulic conductivity Pearson's correlation was performed. Nutrient and DOC balances were calculated from the differences between column outlets and inlet tanks and process rates were calculated dividing nutrient balances by advection time. For these parameters, differences between treatments were analyzed with two factors ANOVA (factor: day and treatment). Differences in DOM properties between treatments were also analyzed with ANOVA (factor: day and treatment). For better understanding the relationship between physic-chemical parameters and biological processes occurring in the columns, values of hydraulic conductivity measured the last day of the experiment were analyzed through ANOVA to detect differences between treatments. Biological data from sediment samples and DO from the last sampling day were analyzed by a two-way ANOVA test for differences between treatments and depths and their interaction. Whenever significant differences

were detected, further Tukey's post hoc tests were performed. Differences between treatments at each depth were further analyzed.

To integrate physic-chemical and biological data along the column, a redundancy analysis (RDA) was performed using one matrix with biofilm biomass and activity values, fitted with another matrix containing physic-chemical parameters (nutrient and DO balances, DOM properties and absolute K values) measured the last day of the experiment in each treatment. Since biofilm biomass and activity was measured at three different depths, data was integrated by depth layers to obtain one number per parameter and treatment. Complementarily, ANOSIM analysis was performed to detect differences between treatments. Further, Pearson's correlation was performed. All statistical analyses were carried out with R statistics (vegan package) excepting ANOSIM analysis which was performed using PRIMER v.6 Software. For multivariate analysis, variables were previously scaled using the scale command in R. For ANOVA analysis all variables were logarithmically transformed to bring the variables close to the normal distribution (Shapiro-Wilk normality test). In all the parameters three replicates were used.

3. Results

3.1 Physicochemical parameters

Flow measured at the start of the experiment was 1.07 ± 0.42 ml/s in Coarse treatment; 0.17 ± 0.03 ml/s and 0.13 ± 0.02 ml/s in Fine-Coarse and in Fine treatments, respectively; 0.39 ± 0.18 ml/s in Coarse-Fine treatment and 0.31 ± 0.1 ml/s in Mixture treatment. Hydraulic conductivity displayed a clear decreasing trend with time (Fig. S1). ANCOVA analysis did not show significant differences in normalized K values between treatments although results showed that in the Coarse and Coarse-fine columns K reduction started later as compared to the other treatments, which showed a sharp reduction in the first days. All columns showed a negative oxygen balance indicating consumption of oxygen from the column inlet to the outlet. Oxygen consumption increased along the experiment reaching values of -6 mg O_2/L at the end of the experiment. Oxygen consumption was correlated with

307 reduction of hydraulic conductivity (Fig. S2) however at the start of the experiment slightly positive
308 oxygen balance values were reported possibly due to still high instability of the system. On the last
309 day of the experiment, the highest K values were measured in treatments displaying coarse sand at
310 the upper layers (Coarse and Coarse-fine treatments, Table 1). Absolute DO values showed a
311 significant decrease in depth ($p < 0.01$, Table 1). The minimum value reported for DO was 2 mg/L.
312 No significant differences in DO were detected between treatments at any given depth but slight
313 oxygen production occurred at the surface of the sediment especially in Fine-Coarse, Fine and
314 Mixture treatment (Table 1). Coarse and Coarse-Fine treatment resulted in high DO consumption rate
315 (Table 2). Coarse treatment showed also the shortest advection time meaning that water passed faster
316 through the sediment. On the other hand, Fine-Coarse and Fine treatments showed the longest
317 advection times indicating more time for water to pass through the sediment (Table 2).

318 After 30 days from the start of the experiment all the ammonium supplied at the inlet (1.26 mg N-
319 NH_4/L) was eventually fully transformed in all treatments (Fig. S3). However, Coarse treatment was
320 showing the highest ammonium consumption rate (Table 2). N-NOx balance showed mainly positive
321 values indicating nitrate/nitrite production. No significant differences were detected between
322 treatments in N-NOx balances, but when analyzing N-NOx production rates Coarse treatment
323 resulted in the highest values (Table 2). Phosphorus was mainly retained through all sediment
324 columns and the highest retention was measured for Fine-Coarse and Fine treatments (Fig. S4). Mean
325 DOC at the inlet tanks was 1.39 ± 0.38 mg/L, at the outlet was 1.44 ± 0.28 mg/L, this results in a very
326 small balance and no differences between treatments were detected.

327 Even though no differences were detected in DOC concentrations differences in DOM properties
328 were reported (Table S1): the Coarse treatment showed the lowest SR and BIX values, while the
329 Coarse-Fine one reported the highest BIX value. E2/E3 values were highest for the Fine-Coarse
330 treatment. The highest BDOC value was observed in the Coarse-fine treatment and the lowest one
331 corresponded to the Fine.

3.2 Sediment biofilm biomass and activity

Bacterial density, chlorophyll and EPS content in sediments showed a strong vertical gradient in depth with highest values at the surface declining sharply in the top 20 cm (Fig. 2). This depth pattern was different depending on the treatment. Bacterial density at the surface was not significantly different between treatments, but at 20 cm depth, the highest values were measured at the Coarse-fine treatment and at 40 cm the highest values were measured at the Coarse treatment. The highest chlorophyll-a concentration at the surface was measured at the Fine-coarse and fine treatment, and at 20 cm depth highest values were found in the Coarse-fine treatment. Mixture treatment showed the lowest EPS concentration at 20 and 40 cm depth.

The LD ratio (live to dead bacteria) was below 1 for all treatments, and increased in depth except in the Coarse treatment (Fig. 3). Functional diversity decreased with depth (Fig. 3); the lowest value was detected in the Coarse column at 20 and 40 cm depths, and the highest was reported for the Fine-coarse column at 20 cm. Analyzing the functional fingerprint, no significant differences were detected between treatments, but that at the surface was different from the ones observed at 20 and 40 cm depth (ANOSIM, $r = 0.567$, $p = 0.0001$).

Extracellular enzyme activities showed a gradient in depth (Table 3). The Coarse-fine treatment showed higher β-glucosidase and β-xylosidase activities in the surface compared to the other sediments. This treatment also showed higher β-xylosidase and phosphatase activities at 20 cm depth. The Coarse treatment showed higher β-glucosidase and leucine-aminopeptidase activities at 40 cm depth.

3.3 Integrating physicochemical and biological responses

Integrating values for each individual column and performing an RDA analysis, data corresponding to biofilm activity, biomass and functional diversity was fitted with the environmental variables (nutrient balances, hydraulic conductivity and DOC properties measured the last day of the experiment) to study the conjunction between biofilm and physical properties (Fig. 4). Treatments

357 displaying coarse sand in the first 20 cm (Coarse and Coarse-fine), are placed on the left of the graph;
358 showing the lowest E2/E3 values and the highest β-glucosidase, β-xylosidase and leucine-
359 aminopeptidase activities. However, differences between the Coarse-fine and the Coarse treatments
360 do exist. The former resulted in higher phosphatase activity, bacterial density, BDOC, BIX, FI, and
361 SR. On the other hand, the Coarse treatment was characterized by highest hydraulic conductivity,
362 lowest phosphorous retention, highest NOx production, and low LD ratio as well as low functional
363 diversity.

364 On the right part of the same graph (Fig.4) we can find the treatments with low hydraulic
365 conductivity (Fine, Fine-coarse and Mixture), all involving fine sand in the upper 20 cm and sharing
366 low values of β-glucosidase, β-xylosidase and leucine-aminopeptidase activities, and high E2/E3
367 values and oxygen consumption. However, interpretation of E2/E3 index should be done cautiously
368 since its values and the tendencies between treatments vary among time. Significant differences were
369 detected between all treatments (ANOSIM, $r = 0.6$, $p = 0.001$), except for Fine and Mixture treatment
370 which could not be discriminated.

371 Pearson's correlations were performed for the last day of the experiment with biological and
372 physicochemical parameters. Significant correlations ($r > 0.5$, $p < 0.05$) are described as follows:
373 hydraulic conductivity was positively correlated with positive balances of N-NOx and phosphorous
374 indicating production of N-NOx and no retention of phosphorous. BDOC was positively correlated
375 with bacterial density. Extracellular enzyme activities were positively correlated between them and
376 bacterial density was positive correlated with all of them. Shannon Index was positively correlated
377 with chl-a content, LD ratio and E2/E3 index. Negative balance of DO was positively correlated with
378 transformation of N-NH4.

379

4. Discussion

4.1 Effects of sediment heterogeneity on physicochemical parameters

Saturated hydraulic conductivity (K) is the most relevant parameter driving flow and transport in porous media. As expected, hydraulic conductivity was highest in the Coarse treatment, while the presence of fine sediments in the other treatments resulted in lower conductivity values. This coincides with Baveye et al.[47] and Pavelic et al.[9] who found higher saturated hydraulic conductivity in coarse-textured materials as compared to fine-textured materials. As expected, high hydraulic conductivity results on high transfer of nutrients, organic matter and DO in depth, which allow for high nitrification rates. Reduction in K as a function of time was mostly associated to biological clogging. However, sharp K reduction at the beginning of the experiment in treatments with fine sediment in the upper layer could be related to sediment compaction[48]. In the columns, reduction of hydraulic conductivity was correlated to oxygen consumption. DO is energetically the most favourable electron acceptor and strongly influences the succession of biogeochemical processes within the subsurface.[49] Specifically, DO is consumed during the mineralization of organic matter and nitrification of ammonium in the oxic zone. However, decrease of oxygen in subsurface sediments could be also related to slow DO supply resulting from the reduction of K and corresponding water fluxes with time.[50] Contrarily to what expecting, no denitrification was achieved in any treatment due to DO concentrations were not low enough. As phosphorous reduction is enhanced by the presence of fine sediment, we expect adsorption to be the main process affecting phosphorous reduction. However, it also could be related to high P uptake by autotrophs,[51] as treatments with fine sediment in the upper part showed high Chl-a concentration at the surface and high phosphorus reduction.

Low SR values reported in the Coarse treatment are indicative of low organic matter degradation (SR values are inversely correlated to organic matter molecular weight).[33] Oppositely, transition from

404 coarse-to-fine sediment could promote biological activity as indicated by high BIX values[35] and high
405 SR values.

406 **4.2 Linking physicochemical parameters to biofilm biomass and activity**

407 In general, biomass and biofilm activity decrease with depth (e.g., Freixa et al.)[52]. This is related to
408 oxygen and nutrients being the limiting factor controlling bacterial growth and metabolic activity[18]
409 and these resources decreasing in depth.[53,54] The experiment show significant interaction between
410 treatment and depth for most biological parameters, indicating that the sediment grain size
411 distribution was affecting differently the activity and biomass patterns in depth.

412 Sediments displaying high hydraulic conductivity values are expected to lead to fast transport of
413 organic matter into deeper sediments[55] due to high infiltration rates. This could explain high bacterial
414 biomass concentrations at large depths in coarse sediments. However, the low proportion of live
415 bacteria in depth and the high reduction on functional diversity in these sediments coincide with less
416 degraded organic matter. Also high leucine-aminopeptidase activity achieved in coarse sediments
417 could be an indicator of organic material released because of cell lysis.[56]

418 The coarse-to-fine transition promotes the accumulation and transformation of organic matter at the
419 interface. This was suggested by the highest capacity to degrade polysaccharides as demonstrated by
420 high C-acquiring enzyme activities, β-glucosidase and β-xylosidase activities. The former is related
421 to cellulose degradation, while the latter is promoted by the presence of hemicellulose.[57] High
422 phosphatase activity in the transition compared to the other treatments could be related to high chl-a
423 content, since algae are also responsible for this activity but may be also linked to low availability of
424 inorganic phosphorus due to its low retention capacity which may enhance bacterial phosphatase
425 activity. High enzyme activities in Coarse-fine treatment coincide with biogeochemical aspects
426 explained above (high BIX and SR values) implying that the coarse-to-fine transition promotes the
427 transformation of organic matter into biodegradable, low-molecular-weight molecules.

In the treatments displaying low hydraulic conductivity, nutrients and organic matter transport to deeper areas are limited, resulting in low microbial activity and biomass in depth. High E2/E3 values measured in such treatments on the last day of the experiment could be indicative of the photo-degradability and photo-reactivity of DOC;[58,59] however this statement should be interpreted with caution since results in E2/E3 index are not consistent throughout the sampling days. High Chl-a concentration measured in these treatments could be favored by high advection time which resulted in slow flow and increased the contact time between water, sediment and light in the upper part of the columns. This in turn could be responsible of slight higher values of DO in the upper part of these columns due to release of oxygen from photosynthetic activity. However, as advection times were much shorter (between 12 minutes and 1 hour) than day/night cycles we expect that the pulses in DO due to algal metabolism will be rapidly dislocated through the columns and then having limited effect on biogeochemical processes. Further work will be necessary to clearly understand specific effects of daily primary production pulses and consequent daily variability on the physicochemical parameters in infiltration systems.

The non-homogeneity of sediment grain size, despite the spatial homogeneity (Mixture treatment) contrarily to what expected, did not favor microbial colonization or extracellular enzyme activity. Furthermore, it resulted in the lowest values of EPS concentration in depth. Since not many differences were accountable between the Fine and the Mixture treatments, we could state that the presence of fine grain size sediments would determine the majority of the biogeochemical processes that take place in the subsurface.

To sum up, sediments composed even partially by coarse sands which display high infiltration rates, transfer high quantity of nutrients and organic matter in depth which promote high bacterial density in deeper areas compared to fine sand sediments. Although not seeing differences in oxygen concentration between treatments; nitrification rates and oxygen consumption rates are greater for coarse sediment. Related to this, higher rates of infiltration may be associated with higher potential

process rates. However, low water residence times in coarse sediments result in low functional diversity and a decrease in the proportion of live bacteria in depth. On the other hand, the presence of fine sands limits biofilm activity and biomass in depth due to low infiltration which at the same time reduce nutrient load in depth. According to this, biofilm activity, biomass and process rates could be limited by low nutrient load. On the other hand, phosphorous retention is enhanced by fine sediment. Transition of coarse to fine grain size sediments promote the accumulation of organic matter in the interface, favoring its decomposition to smaller and more biodegradable compounds and creating hot-spots of bacterial activity and biomass.

The present work concludes that biological and physicochemical parameters are influenced by the grain size and the grain size distribution of the sediment. In relation to our hypothesis, coarse sediment allows for high biomass in depth and high process rates due to high input load, while fine sediment promotes accumulation of algae in the upper part of the columns and ameliorates phosphorous retention but biomass in subsurface is constrained by low input loads. However, in contrast to our hypothesis mixture of coarse and fine sediment behaves similarly than only fine sediment. Interestingly, bilayer of coarse sediment in the upper part and fine sediment in the bottom promotes high biomass in the interface between the two layers resulting in high microbial organic matter degradation and nutrient recycling and also allows for phosphorous retention mainly thanks to the fine layer.

In short, it is important to account for the implications of grain size and spatial transitions between layers in subsurface sediments in order to understand and improve biological and physical knowledge about processes occurring either in natural or in artificial infiltration systems. It is important to take into account that implications of sediment heterogeneity on microbial biomass and activity are not fully characterized by the topsoil few cm, but rather influenced by the grain size spatial distribution of at least the top 40 cm.

Supporting Information

The supporting information is available free of charge via the Internet at http://pubs.acs.org. DOM properties measured in each treatment during the experiment (Table S1), temporal variation of normalized hydraulic conductivity for each treatment (Figure S1), relationship between oxygen balance and normalized hydraulic conductivity (Figure S2), temporal variation of ammonium, nitrate, and nitrite balances (Figure S3), temporal variation of phosphorous balance (Figure S4).

Acknowledgements

This work was supported by European Union [project MARSOL, grant number 619120], Spanish Ministry of Economy and Competitiveness [CGL2014-58760-C3-2-R], Department of Universitats, Recerca i Societat de la Informació de la Generalitat de Catalunya, and European Social Fund . XS acknowledges support from the Icrea Academia Program.

References

(1) Findlay, S., Sinsabaugh, R., 2003. Response of hyporheic biofilm metabolism and community structure to nitrogen amendments. Aquat. Microb. Ecol. 33, 127–136.

(2) Romaní, A., Giorgi, A., Acuña, V., Sabater, S., 2004. The influence of substratum type and nutrient supply on biofilm organic matter utilization in streams. Limnol. Oceanogr. 49, 1713–1721.

(3) Bekele, E., Toze, S., Patterson, B., Higginson, S., 2011. Managed aquifer recharge of treated wastewater: Water quality changes resulting from infiltration through the vadose zone. Water Res. 45, 5764–5772. doi:10.1016/j.watres.2011.08.058.

(4) Dillon, P., Page, D., Vanderzalm, J., Pavelic, P., Toze, S., Bekele, E., Sidhu, J., Prommer, H., Higginson, S., Regel, R., Rinck-Pfeiffer, S., Purdie, M., Pitman, C., Wintgens, T., 2008. A critical evaluation of combined engineered and aquifer treatment systems in water recycling. Water Sci. Technol. 57, 753–762. doi:10.2166/wst.2008.168.

(5) Miller, J.H., Ela, W.P., Lansey, K.E., Chipello, P.L., Arnold, R.G., 2009. Nitrogen Transformations during Soil–Aquifer Treatment of Wastewater Effluent—Oxygen Effects in Field Studies. J. Environ. Eng. 132, 1298–1306. doi:10.1061/ASCE0733-93722006132:101298.

(6) Greskowiak, J., Prommer, H., Massmann, G., Johnston, C.D., Nützmann, G., Pekdeger, A., 2005. The impact of variably saturated conditions on hydrogeochemical changes during artificial recharge of groundwater. Appl. Geochemistry 20, 1409–1426. doi:10.1016/j.apgeochem.2005.03.002.

(7) Pedretti, D., Barahona-Palomo, M., Bolster, D., Sanchez-Vila, X., & Fernàndez-Garcia, D. (2012). A quick and inexpensive method to quantify spatially variable infiltration capacity for artificial recharge ponds using photographic images. Journal of hydrology, 430, 118-126.

(8) Türkmen, M., Walther, E.F., Andres, A.S., Chirnside, A.A.E., Ritter, W.F., 2008. Evaluation of rapid infiltration basin systems (RIBS) for wastewater disposal: Phase I.

(9) Pavelic, P., Dillon, P.J., Mucha, M., Nakai, T., Barry, K.E., Bestland, E., 2011. Laboratory assessment of factors affecting soil clogging of soil aquifer treatment systems. Water Res. doi:10.1016/j.watres.2011.03.027.

(10) Cunningham, A.B., Characklis, W.G., Abedeen, F., Crawford, D., 1991. Influence of Biofilm Accumulation on Porous Media Hydrodynamics. Environ. Sci. Technol. 25, 1305–1311.

(11) Rodríguez-Escales, P., Sanchez-Vila, X. (2016). Fate of sulfamethoxazole in groundwater: Conceptualizing and modeling metabolite formation under different redox conditions. Water Research, 105, 540-550. Doi: 10.1016/j.watres.2016.09.034.

(12) Romaní, A.M., Artigas, J., Ylla, I., 2012. Extracellular Enzymes in Aquatic Biofilms: Microbial Interactions versus Water Quality Effects in the Use of Organic Matter, in: Lear, G., Lewis, G.. (Eds.), Microbial Biofilms. Caister Academic Press, UK, pp. 153–174.

(13) Sutherland, I. W. (1985). Biosynthesis and composition of gram-negative bacterial extracellular

526 and wall polysaccharides. Annual Reviews in Microbiology, 39(1), 243-270.

527 (14) Rinck-Pfeiffer, S., Ragusa, S., Sztajnbok, P., Vandevelde, T., 2000. Interrelationships between
528 biological, chemical, and physical processes as an analog to clogging in aquifer storage and
529 recovery (ASR) wells. Water Res. 34, 2110–2118. doi:10.1016/S0043-1354(99)00356-5.

530 (15) Okubo, T., and Matsumoto, J. (1979). Effect of infiltration rate on biological clogging and water
531 quality changes during artificial recharge. Water Resources Research, 15(6), 1536-1542.

532 (16) Or, D., Phutane, S., Dechesne, A., 2007a. Extracellular Polymeric Substances Affecting Pore-
533 Scale Hydrologic Conditions for Bacterial Activity in Unsaturated Soils. Vadose Zo. J. 6, 298–
534 305.

535 (17) Rodríguez-Escales, P., Folch, A., van Breukelen, B.M., Vidal-Gavilan, G., Sanchez-Vila, X.
536 (2016). Modeling long term Enhanced in situ Biodenitrification and induced heterogeneity in
537 column experiments under different feeding strategies. Journal of Hydrology, 538, 127–137.
538 Doi: 10.1016/j.jhydrol.2016.04.012.

539 (18) Battin, T.J., Sengschmitt, D., 1999. Linking Sediment Biofilms, Hydrodynamics, and River Bed
540 Clogging: Evidence from a Large River. Microb. Ecol. 37, 185–196.
541 doi:10.1007/s002489900142.

542 (19) Rubol, S., Freixa, A., Carles-Brangari´, A., Ferna`ndez-Garcia, D., Romani´, A.M., Sanchez-
543 Vila, X., 2014. Connecting bacterial colonization to physical and biochemical changes in a sand
544 box infiltration experiment. J. Hydrol. doi:10.1016/j.jhydrol.2014.05.041.

545 (20) Or, D., Smets, B.F., Wraith, J.M., Dechesne, A., Friedman, S.P., 2007b. Physical constraints
546 affecting bacterial habitats and activity in unsaturated porous media – a review. Adv. Water
547 Resour. 30, 1505–1527. doi:10.1016/j.advwatres.2006.05.025.

548 (21) Wang, S.-Y., Sudduth, E.B., Wallenstein, M.D., Wright, J.P., Bernhardt, E.S., 2011. Watershed
549 urbanization alters the composition and function of stream bacterial communities. PLoS One 6,

1–9. doi:10.1371/journal.pone.0022972.

(22) Nogaro, G., Datry, T., Mermillod-Blondin, F., Descloux, S., Montuelle, B., 2010. Influence of streambed sediment clogging on microbial processes in the hyporheic zone. Freshw. Biol. 55, 1288–1302. doi:10.1111/j.1365-2427.2009.02352.x.

(23) Mermillod-Blondin, F., Mauclaire, L., Montuelle, B., 2005. Use of slow filtration columns to assess oxygen respiration, consumption of dissolved organic carbon, nitrogen transformations, and microbial parameters in hyporheic sediments. Water Res. 39, 1687–1698. doi:10.1016/j.watres.2005.02.003.

(24) Boulton, A.J., Findlay, S., Marmonier, P., Stanley, E.H., Valett, H.M., 1998. The Functional Significance of the Hyporheic Zone in Streams and Rivers. Annu. Rev. Ecol. Syst. 29, 59–81. doi:10.1146/annurev.ecolsys.29.1.59.

(25) Fuchs, S.,Hahn, H.H., Roddewig, J., Schwarz, M., Turkovic, R., 2004. Biodegradation and Bioclogging in the Unsaturated Porous Soil benath Sewer Leaks. Acta Hydrochim.hydrobiol. 32, 277-286. Doi:10.1002/aheh.200400540

(26) Malard, F., Tockner, K., Dole-Olivier, M.J., Ward, J. V., 2002. A landscape perspective of surface-subsurface hydrological exchanges in river corridors. Freshw. Biol. 47, 621–640. doi:10.1046/j.1365-2427.2002.00906.x.

(27) Higashino, M., 2013. Quantifying a significance of sediment particle size to hyporheic sedimentary oxygen demand with a permeable stream bed. *Environ. Fluid Mech*, *13*(3), 227-241.

(28) Essandoh, H.M.K., Tizaoui, C., Mohamed, M.H.A., 2013. Removal of dissolved organic carbon and nitrogen during simulated soil aquifer treatment. Water Res. 47, 3559–3572. doi:10.1016/j.watres.2013.04.013.

(29) Dodds, W. K., Randel, C. A., & Edler, C. C. (1996). Microcosms for aquifer research:

574 application to colonization of various sized particles by ground-water microorganisms. *Ground*
575 *Water*, *34*(4), 756.

576 (30) Ylla, I., Romaní, A. M., & Sabater, S. (2012). Labile and recalcitrant organic matter utilization
577 by river biofilm under increasing water temperature. Microb. Ecol. 64(3), 593-604.

578 (31) Murphy, J., and Riley, J. (1962). A modified single solution method for the determination of
579 phosphate in natural waters. Analytica chimica acta,27, 31-36.

580 (32) Reardon, J., Foreman, J. A., & Searcy, R. L. (1966). New reactants for the colorimetric
581 determination of ammonia. Clinica Chimica Acta, 14(3), 403-405.

582 (33) Helms, J.R., Stubbins, A., Ritchie, J.D., Minor, E.C., Kieber, D.J., Mopper, K., 2008.
583 Absorption spectral slopes and slope ratios as indicators of molecular weight, source, and
584 photobleaching of chromophoric dissolved organic matter. Limonology Oceanogr. 53, 955–969.
585 doi:10.4319/lo.2008.53.3.0955.

586 (34) Cory, R.M., Mcknight, D.M., 2005. Fluorescence Spectroscopy Reveals Ubiquitous Presence of
587 Oxidized and Reduced Quinones in Dissolved Organic Matter Fluorescence Spectroscopy
588 Reveals Ubiquitous Presence of Oxidized and Reduced Quinones in Dissolved Organic Matter.
589 Environ. Sci. Technol. 39, 8142–8149. doi:10.1021/es0506962.

590 (35) Huguet, A., Vacher, L., Relexans, S., Saubusse, S., Froidefond, J.M., Parlanti, E., 2009.
591 Properties of fluorescent dissolved organic matter in the Gironde Estuary. Org. Geochem. 40,
592 706–719. doi:10.1016/j.orggeochem.2009.03.002.

593 (36) Minero, C., Lauri, V., Falletti, G., Maurino, V., Pelizzetti, E., Vione, D., 2007.
594 Spectrophotometric characterisation of surface lakewater samples: implications for the
595 quantification of nitrate and the properties of dissolved organic matter. Ann. Chim. 97, 1107–
596 1116.

597 (37) Servais, P., Anzil, A., Ventresque, C., 1989. Simple Method for Determination of Biodegradable

598 Dissolved Organic Carbon in Water. Appl. Environ. Microbiol. 55, 2732–2734. doi:0099-
599 2240/89/102732-03.

600 (38) Amalfitano, S., Fazi, S., Puddu, A., 2009. Flow cytometric analysis of benthic prokaryotes
601 attached to sediment particles. J. Microbiol. Methods 79, 246–249.
602 doi:10.1016/j.mimet.2009.09.005.

603 (39) Quéric, N. V., Soltwedel, T., Arntz, W.E., 2004. Application of a rapid direct viable count
604 method to deep-sea sediment bacteria. J. Microbiol. Methods 57, 351–367.
605 doi:10.1016/j.mimet.2004.02.005.

606 (40) Amalfitano, S., Fazi, S., 2008. Recovery and quantification of bacterial cells associated with
607 streambed sediments. J. Microbiol. Methods 75, 237–243. doi:10.1016/j.mimet.2008.06.004.

608 (41) Falcioni, T., Manti, A., Boi, P., Canonico, B., Balsamo, M., Papa, S., 2006. Comparison of
609 Disruption Procedures for Enumeration of Activated Sludge Floc Bacteria by Flow Cytometry.
610 Cytom. Part B Clin. Cytom. 70B, 149–153. doi:10.1002/cyto.b.20097

611 (42) Boulos, L., Prévost, M., Barbeau, B., Coallier, J., Desjardins, R., 1999. Methods LIVE / DEAD
612 ® Bac Light E : application of a new rapid staining method for direct enumeration of viable and
613 total bacteria in drinking water. J. Microbiol. Methods 37, 77–86.

614 (43) Jeffrey, S.W., & Humphrey, G.F. (1975). New spectrophotometric equations for determining
615 chlorophylls a, b, c1 and c2 in higher plants, algae and natural phytoplankton. Biochemie und
616 Physiologie der Pflanzen 167, 191-194.

617 (44) Dubois, M., Gilles, K. a., Hamilton, J.K., Rebers, P. a., Smith, F., 1956. Colorimetric method for
618 determination of sugars and related substances. Anal. Chem. 28, 350–356.
619 doi:10.1021/ac60111a017.

620 (45) Romaní, A., Sabater, S., 2000. Influence of Algal Biomass on Extracellular Enzyme Activity in
621 River Biofilms. Microb. Ecol. 41, 16–24. doi:10.1007/s002480000041.

622 (46) Magurran, A.E. (1988). Diversity indices and species abundance models. In: Ecological
623 Diversity and Its measurement. 7-45, Springer, Netherlands.

624 (47) Baveye, P., Vandevivere, P., Hoyle, B.L., DeLeo, P.C., de Lozada, D.S., 1998. Environmental
625 Impact and Mechanisms of the Biological Clogging of Saturated Soils and Aquifer Materials.
626 Crit. Rev. Environ. Sci. Technol. 28, 123–191. doi:10.1080/10643389891254197.

627 (48) Hoffman, F., Ronen, D., & Pearl, Z. (1996). Evaluation of flow characteristics of a sand column
628 using magnetic resonance imaging. J. Contam. Hydrol. 22(1-2), 95-107.

629 (49) Baker, M. A., Valett, H. M., & Dahm, C. N. (2000). Organic carbon supply and metabolism in a
630 shallow groundwater ecosystem. Ecology, 81(11), 3133-3148.

631 (50) Martienssen, M., & Schöps, R. (1997). Biological treatment of leachate from solid waste landfill
632 sites—alterations in the bacterial community during the denitrification process. Water Res.
633 31(5), 1164-1170.

634 (51) Jarvie, H. P., Neal, C., Warwick, A., White, J., Neal, M., Wickham, H. D., Hill, L.K., &
635 Andrews, M. C. (2002). Phosphorus uptake into algal biofilms in a lowland chalk river. Science
636 of the Total Environment 282, 353-373.

637 (52) Freixa, A., Rubol, S., Carles-Brangarí, A., Fernàndez-Garcia, D., Butturini, A., Sanchez-Vila,
638 X., Romaní, A., 2016. The effects of sediment depth and oxygen concentration on the use of
639 organic matter: An experimental study using an infiltration sediment tank. Sci. Total Environ.
640 540, 20–31. doi:10.1016/j.scitotenv.2015.04.007.

641 (53) Hall, E.K., Besemer, K., Kohl, L., Preiler, C., Riedel, K., Schneider, T., Wanek, W., Battin, T.J.,
642 2012. Effects of resource chemistry on the composition and function of stream hyporheic
643 biofilms. Front. Microbiol. 3, 1–14. doi:10.3389/fmicb.2012.00035.

644 (54) Nogaro, G., Datry, T., Mermillod-Blondin, F., Foulquier, A., Montuelle, B., 2013. Influence of
645 hyporheic zone characteristics on the structure and activity of microbial assemblages. Freshw.

646 Biol. 58, 2567–2583. doi:10.1111/fwb.12233.

647 (55) Rauch-Williams, T., Drewes, J.E., 2006. Using soil biomass as an indicator for the biological
648 removal of effluent-derived organic carbon during soil infiltration. Water Res. 40, 961–968.
649 doi:10.1016/j.watres.2006.01.007.

650 (56) Ricart, M., Barceló, D., Geiszinger, A., Guasch, H., de Alda, M. L., Romaní, A. M., Vidal, G.,
651 Villagrasa, M., Sabater, S. (2009). Effects of low concentrations of the phenylurea herbicide
652 diuron on biofilm algae and bacteria. Chemosphere, 76(10), 1392-1401.

653 (57) Sabater, S., and Romaní, A.M. (1996). Metabolic changes associated with biofilm formation in
654 an undisturbed Mediterranean stream. Hydrobiologia, 335(2), 107-113.

655 (58) Chow, A.T., Dai, J., Conner, W.H., Hitchcock, D.R., Wang, J.J., 2013. Dissolved organic matter
656 and nutrient dynamics of a coastal freshwater forested wetland in Winyah Bay, South Carolina.
657 Biogeochemistry 112, 571–587. doi:10.1007/s10533-012-9750-z.

658 (59) Macdonald, M.J., Minor, E.C., 2013. Photochemical degradation of dissolved organic matter
659 from streams in the western Lake Superior watershed. Aquat. Sci. 75, 509–522.
660 doi:10.1007/s00027-013-0296-5.

661

Figures & Tables

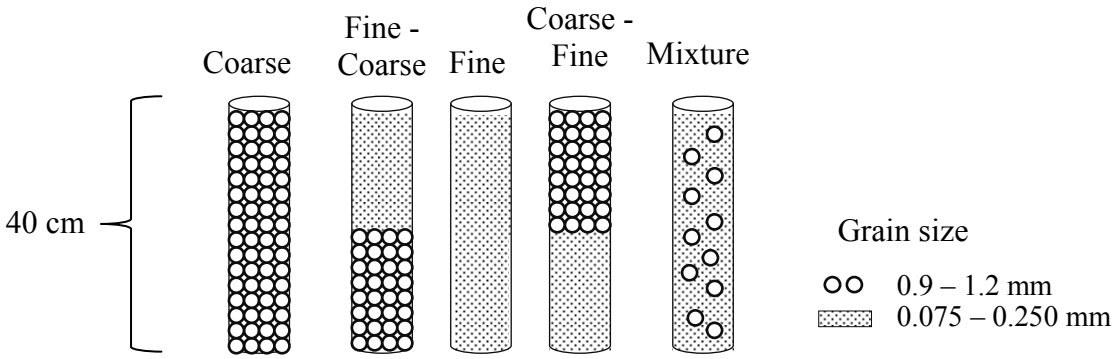

Figure 1 Scheme of the column configurations regarding grain size distributions used in this experiment. Three replicate columns were used for each treatment.

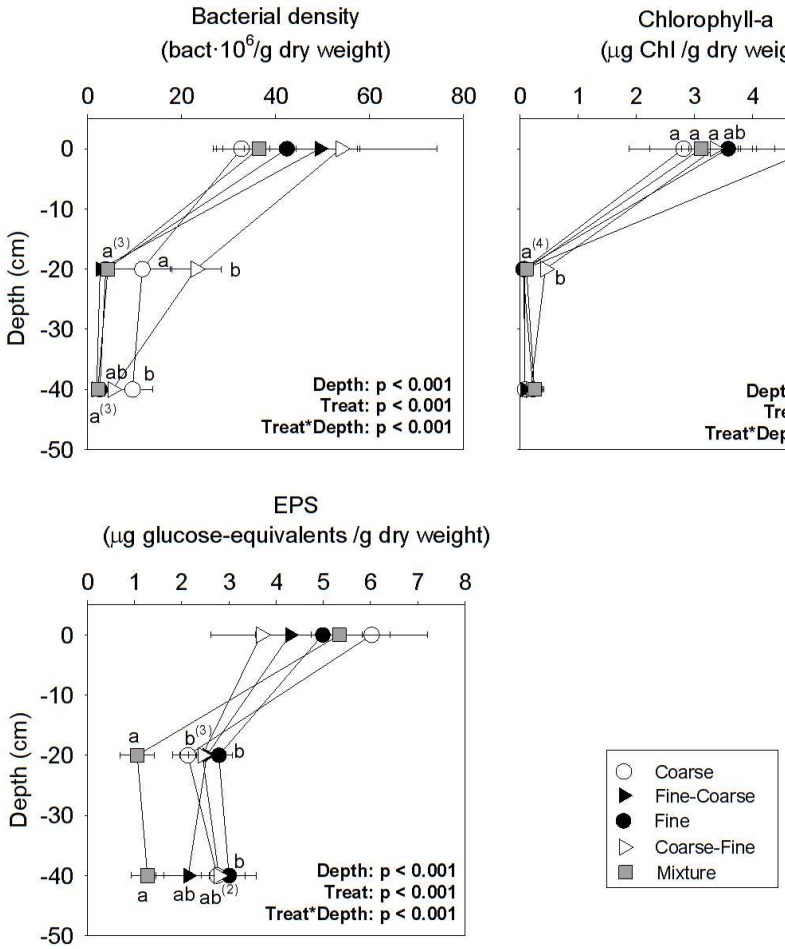

Figure 2 Absolute values of biofilm biomass (bacterial density; chlorophyll-a content and EPS content) measured in sediment at different depths at the end of the experiment. Letters indicate significant differences between treatments (Treat) on each depth after Tukey's post-hoc analysis. Superscripts indicate the number of treatments in the same group.

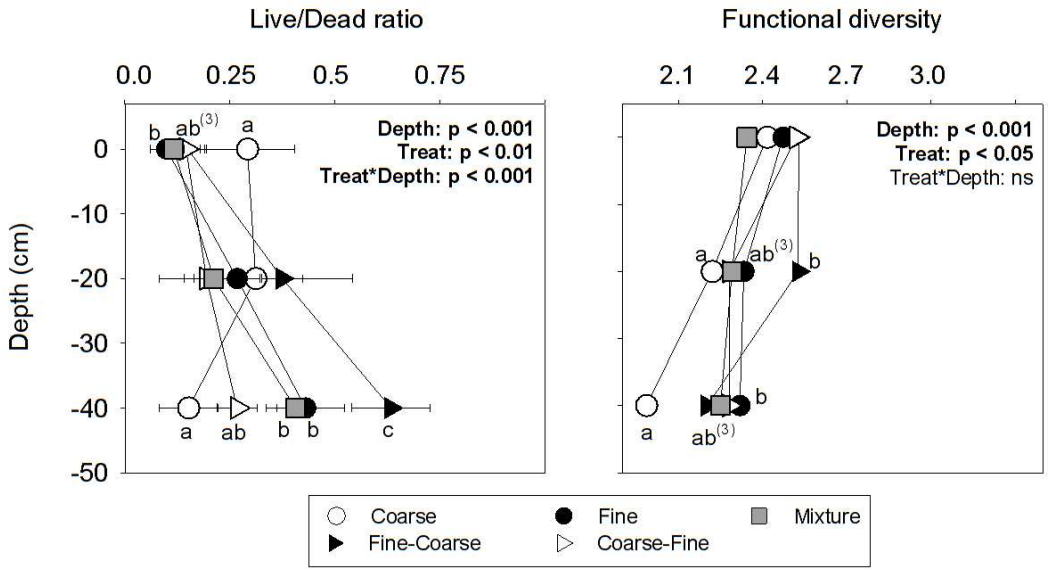

671

672 **Figure 3** LD ratio values and functional diversity measured as Shannon diversity. Letters indicate significant
673 differences between treatments (Treat) on each depth after Tukey's post-hoc analysis. Superscripts indicate the
674 number of treatments in the same group.

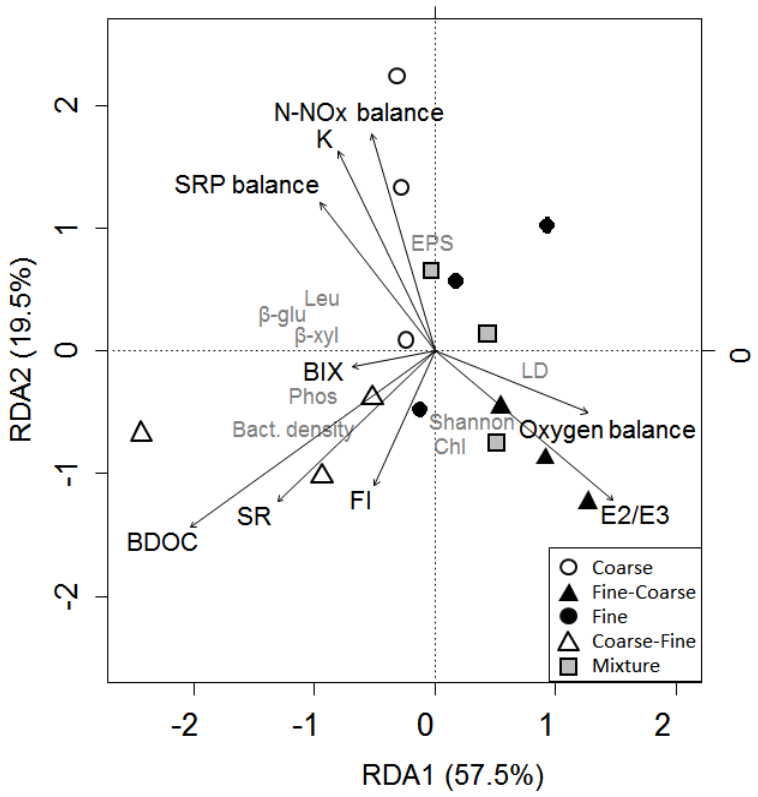

675

676 **Figure 4** RDA analysis with data from sediment biofilm fitted with physicochemical data from the last day of
677 the experiment. ANOSIM analysis detect differences between treatments (ANOSIM R = 0.604, p = 0.001).

678 **Table 1** Hydraulic conductivity and dissolved oxygen measured the last day of the experiment in each
679 treatment

	K (m/day)	O_2 surface (mg/L)	O_2 – 20 cm (mg/L)	O_2 – 40 cm (mg/L)
Coarse	**0.3078^{b}** ± *0.1086*	5.46 ± *0.78*	3.86 ± *0.13*	2.92 ± *0.44*
Fine – coarse	0.1019^{a} ± *0.0602*	7.75 ± *2.90*	5.43 ± *4.10*	3.44 ± *2.27*
Fine	0.1319^{a} ± *0.0505*	8.22 ± *3.68*	3.47 ± *0.71*	1.91 ± *0.73*
Coarse – fine	0.1867^{ab} ± *0.1133*	5.84 ± *0.85*	2.98 ± *0.35*	2.15 ± *0.74*
Mixture	0.1120^{a} ± *0.0334*	8.66 ± *0.19*	4.86 ± *1.29*	3.33 ± *0.85*

680 Values are the mean of the replicates (n=3) ± sd. Letters next to the means indicate significant different groups
681 after Tukey's post-hoc analysis ($p < 0.05$).

682 **Table 2** Advection time and process rates for ammonium, nitrates and nitrites (NOx), phosphorous (SRP) and
683 dissolved oxygen (DO) along the infiltration columns

	Advection time (seconds)	N-NH4 (µg N/L·s)	N-NOx (µg N/L·s)	SRP (µg P/L·s)	DO (µg O2/L·s)
Day	**p < 0.001**	**p < 0.001**	**p < 0.001**	**p < 0.001**	**p < 0.001**
Treat	**p < 0.001**	**p < 0.001**	**p < 0.001**	**p < 0.001**	**p < 0.001**
Treat*day	ns	**p < 0.001**	**p < 0.001**	**p < 0.001**	**p < 0.01**
Coarse	736^{a} ± *700*	-1.70^{b} ± *1.17*	2.14^{b} ± *1.61*	0.0007^{a} ± *0.0380*	-5.05^{c} ± *1.61*
Fine - Coarse	3890^{c} ± *2313*	-0.36^{a} ± *0.10*	0.22^{a} ± *0.29*	-0.0181^{b} ± *0.0222*	-0.82^{a} ± *0.83*
Fine	2500^{bc} ± *1482*	-0.52^{a} ± *0.23*	0.38^{a} ± *0.29*	-0.0231^{b} ± *0.0299*	-1.53^{ab} ± *1.50*
Coarse – Fine	1577^{ab} ± *1160*	-0.75^{a} ± *0.43*	0.63^{a} ± *0.73*	-0.0142^{b} ± *0.0170*	-2.03^{b} ± *2.00*
Mixture	2029^{ab} ± *1231*	-0.49^{a} ± *0.15*	0.49^{a} ± *0.19*	-0.0124^{b} ± *0.0177*	-1.01^{ab} ± *1.20*

684 Values are the mean of the four sampling days (n = 12) ± sd. Positive process rates indicate production while
685 negative process rates means removal/consumption. Letters next to the means indicate significant differences
686 between treatments (Treat) after Tukey's post-hoc analysis.

687

688 **Table 3** Enzyme activities measured at different depths in each treatment

	Depth (cm)	Coarse	Fine - coarse	Fine	Coarse - fine	Mixture
β-glu	0	3.90^{ab} ± *0.28*	2.30^{a} ± *0.92*	2.39^{a} ± *0.13*	**7.39^{b}** ± *1.51*	3.93^{ab} ± *0.04*
Depth: p < 0.001	20	1.32 ± *0.56*	0.32 ± *0.38*	0.71 ± *0.75*	2.30 ± *1.73*	0.84 ± *0.79*
Treat: p < 0.001	40	**1.08^{b}** ± *0.58*	0.15^{a} ± *0.12*	0.48^{a} ± *0.35*	0.42^{a} ± *0.04*	0.38^{a} ± *0.12*
Treat*Depth: ns						
β-xyl	0	1.14^{ab} ± *0.39*	0.61^{a} ± *0.51*	1.06^{ab} ± *0.37*	**1.22^{b}** ± *0.45*	0.66^{a} ± *0.24*
Depth: p < 0.001	20	0.17^{ab} ± *0.14*	0.01^{a} ± *0.02*	0.06^{a} ± *0.11*	**0.90^{b}** ± *0.74*	0.07^{a} ± *0.13*
Treat: p < 0.001	40	0.10 ± *0.09*	0.00 ± *0.00*	0.02 ± *0.03*	0.18 ± *0.31*	0.00 ± *0.00*
Treat*Depth: ns						
Phos	0	6.20 ± *0.29*	12.31 ± *3.68*	8.69 ± *2.91*	9.56 ± *1.01*	9.88 ± *2.95*
Depth: p < 0.001	20	3.36^{a} ± *0.57*	2.24^{a} ± *0.30*	3.38^{a} ± *2.43*	**6.06^{b}** ± *1.63*	2.81^{a} ± *0.57*
Treat: p < 0.05	40	2.31^{ab} ± *0.69*	1.14^{a} ± *0.28*	2.41^{ab} ± *0.76*	**3.86^{b}** ± *0.89*	1.98^{ab} ± *0.56*
Treat*Depth: ns						
Leu	0	4.10 ± *0.58*	5.84 ± *2.94*	6.40 ± *3.09*	7.43 ± *0.83*	2.58 ± *0.66*
Depth: p < 0.001	20	**4.86^{b}** ± *0.84*	1.96^{a} ± *1.12*	2.52^{ab} ± *1.14*	3.98^{ab} ± *0.95*	3.28^{ab} ± *0.78*
Treat: p < 0.05	40	**4.42^{b}** ± *0.59*	1.18^{a} ± *0.41*	1.73^{a} ± *1.01*	3.37^{ab} ± *1.78*	1.59^{a} ± *0.98*
Treat*Depth: p < 0.1						

689 Values are the mean of the replicates (n=3) ± sd, expressed as nmolMUF/g dry weight·h for β-glucosidase (β-
690 glu), β-xylosidase (β-xyl) and Phosphatase (Phos); and nmolAMC/g dry weight·h for Leucine-aminopeptidase
691 (Leu). Letters next to the means indicate significant differences between treatments (Treat) after Tukey's post-
692 hoc analysis comparing treatments at each depth. Values in bold indicate the highest activity measured at each
693 depth.